



Cite this: *Chem. Commun.*, 2014, 50, 14504

Received 25th August 2014,  
Accepted 29th September 2014

DOI: 10.1039/c4cc06696k

www.rsc.org/chemcomm

**Pressure-driven orbital reordering in the quantum magnet  $[(\text{CuF}_2(\text{H}_2\text{O})_2)_x(\text{pyz})]^\dagger$  ( $\text{pyz} = \text{pyrazine}$ ), dramatically affects its magnetic exchange interactions. The crystal chemistry of this system is enriched with a new phase above 3 GPa, surprisingly concomitant with other polymorphs. Moreover, we discovered an unprecedented compound with a different stoichiometry,  $[(\text{CuF}_2(\text{H}_2\text{O})_2)_2(\text{pyz})]$ , featuring magnetic bi-layers.**

In the past few years,  $[(\text{CuF}_2(\text{H}_2\text{O})_2)(\text{pyz})]$  (**1**) has been extensively investigated due to its rapidly evolving phase diagram as a function of pressure and, consequently, an easy control of its magnetism.<sup>1–3</sup> In the monoclinic  $P2_1/c$  ambient pressure structure,  $\alpha$ -**1**,<sup>4</sup> the three ligands pairwise occupy the *trans* positions of a distorted octahedron around Cu. By connecting pairs of  $\text{Cu}^{2+}$  ions, the pyrazine ligands build a mono-dimensional (1D) coordination polymer along the crystallographic *a* axis. These chains pack in a tight 2D supramolecular network of  $\text{O}-\text{H}\cdots\text{F}$  hydrogen bonds expanded in the *bc* plane (Fig. 1) producing a quasi-2D magnetic network.<sup>2</sup> The N–Cu bonds are rather elongated, *i.e.* they produce a pseudo Jahn–Teller axis.<sup>5</sup> This implies that the singly occupied d orbital of Cu (the magnetic orbital) is perpendicular to this direction and thus involves  $\text{H}_2\text{O}$  and  $\text{F}^-$  but not  $\text{pyz}$  (as confirmed by the spin density maps we calculated, Fig. S3 in ESI†). A previous powder X-ray diffraction (P-XRD) study<sup>2</sup> has shown that **1** undergoes two successive, pressure-induced, isosymmetric phase transitions of the first order, both of which switch the stretched Cu–X bond direction, implying an *orbital reordering*. In fact, at around 1 GPa, phase transition I (see Scheme 1) produces  $\beta$ -**1**, whose octahedron is elongated along the  $\text{H}_2\text{O}-\text{Cu}-\text{OH}_2$  direction. Water molecules no longer interact with the magnetic orbital

## New magnetic frameworks of $[(\text{CuF}_2(\text{H}_2\text{O})_2)_x(\text{pyz})]^\dagger$

A. Lanza,<sup>ab</sup> C. Fiolka,<sup>a</sup> M. Fisch,<sup>ab</sup> N. Casati,<sup>b</sup> M. Skoulatos,<sup>c</sup> C. Rüegg,<sup>cd</sup>  
K. W. Krämer<sup>a</sup> and Piero Macchi<sup>\*a</sup>

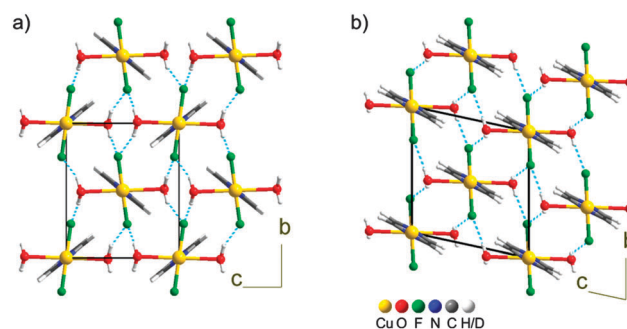
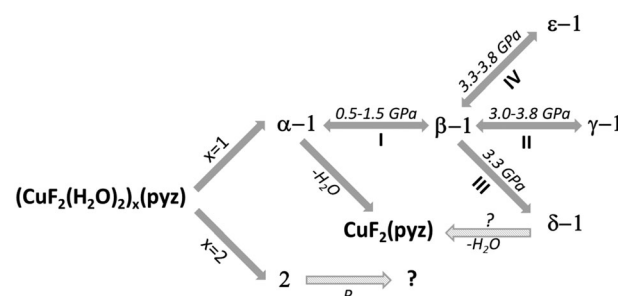


Fig. 1 Comparison between the crystal packing of **1** in phases  $\beta$  (a) and  $\epsilon$  (b). The hydrogen bond network in the *bc* plane is shown with blue dashed lines.



Scheme 1 Transformations in the  $[(\text{CuF}_2(\text{H}_2\text{O})_2)_x(\text{pyz})]$  system.

(Fig. S4, ESI†) and therefore the exchange path is just 1D, propagating along the Cu–pyz–Cu chains. A second phase transition (II, in Scheme 1) was observed at around 3.3 GPa yielding  $\gamma$ -**1**, for which the Cu–F bonds are now elongated.<sup>2</sup> Although the structure of  $\gamma$ -**1** has been refined only using a very rigid model and the magnetism has not been investigated, it was sensibly assumed that the magnetic orbital lies in the  $\text{Cu}(\text{pyz})_2(\text{H}_2\text{O})_2$  plane, hindering the coupling of magnetic centers through the H-bonds and maintaining the same  $\beta$ -**1**-type 1D network. This sequence of phase transitions replicates the spectrochemical series of the ligands ( $\text{pyz} > \text{H}_2\text{O} > \text{F}^-$ ).

On the other hand, in a more recent single crystal X-ray diffraction (SC-XRD) study, Prescimone *et al.*<sup>3</sup> identified a new

<sup>a</sup> Department of Chemistry and Biochemistry, University of Bern, Freiestrasse 3, 3012 Bern, Switzerland

<sup>b</sup> Swiss Light Source, Paul Scherrer Institute, CH-5232 Villigen, Switzerland

<sup>c</sup> Laboratory for Neutron Scattering and Imaging, Paul Scherrer Institute, CH-5232 Villigen, Switzerland

<sup>d</sup> DPMC-MaNEP, University of Geneva, CH-1211 Geneva, Switzerland

† Electronic supplementary information (ESI) available: Detailed experimental section and results. CCDC 998110 and 998111. For the ESI and crystallographic data in CIF or other electronic format see DOI: 10.1039/c4cc06696k



triclinic phase ( $\delta$ -1) at 3.3 GPa after a first order phase transition (III, in Scheme 1).  $\delta$  significantly differs from  $\alpha$ ,  $\beta$  or  $\gamma$  as it features Cu–F–Cu bridges obtained from the nucleophilic substitution by a fluoride ligand on one water molecule, which leaves the Cu coordination sphere and occupies an extra-framework site. The elongated direction of the Cu octahedron is  $F_{\text{bridge}}\text{--Cu--H}_2\text{O}$ , an intermediate step along the spectrochemical series. At variance with I and II, reversibility of transition III has not been reported and is very likely impossible.

In order to explore the rich solid-state chemistry of **1**, we undertook a study aimed at explaining the factors governing the dichotomy at 3.3 GPa. In fact, the powder experiments described in ref. 2 were carried out using isopropanol as the pressure transmitting medium (PTM), whereas for the single crystal experiments described in ref. 3, petrol ether was used. Thus, we performed extensive X-ray diffraction investigations on single crystal and powder samples using different PTMs. For most experiments we used crystals of the fully deuterated compound, but in order to maintain consistency and fluency throughout the manuscript we will not explicitly distinguish

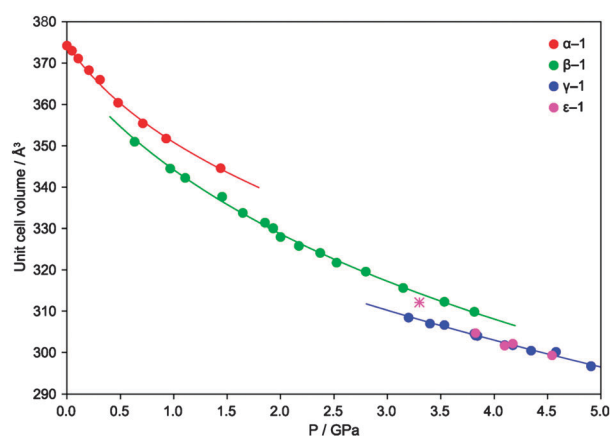


Fig. 2 The unit cell volume of phases of **1** as a function of  $P$ , obtained from P-XRD experiments in different PTMs and using different pressure increase rates and equilibration times. The volume of  $\epsilon$ -1 obtained from the SC-XRD is marked as a star. The lines represent the fitted equations of state. Error bars are smaller than the markers.

H from D, unless necessary. All experiments confirmed the occurrence of phase transition I, in a rather large pressure range at around 1.0 GPa (Fig. 2) with co-existence of  $\beta$ -1 and  $\alpha$ -1, depending on the experimental conditions, in particular on the pressure increase rate (*i.e.*  $\Delta P/\Delta t$ , where  $\Delta P$  is the pressure increase and  $\Delta t$  is the time between one measurement and the next, including equilibration). Upon further compression, we discovered and characterized by SC-XRD a new polymorph,  $\epsilon$ -1, obtained from  $\beta$ -1 at *ca.* 3.3 GPa, which is the same pressure previously reported for the occurrence of both  $\gamma$ -1 and  $\delta$ -1. This transformation (IV, in Scheme 1) is also a first order phase transition, reproducible under several conditions.

In  $\epsilon$ -1, the intra- and inter-molecular connectivity of  $\beta$ -1 is retained, although the symmetry is lowered to triclinic (Table 1).<sup>6</sup> The asymmetric unit comprises one copper ion, located at an inversion center, one water molecule, one fluoride and half pyz, building a distorted octahedron. The distinctive feature of  $\epsilon$ -1 is the reorientation of the pyz rings, which are all parallel to each other within the chain and among neighboring chains, whereas, in all other known phases of **1**, neighboring chains alternate two orientations. The compression also causes the pyz planes to deviate from the Cu...Cu direction, forming an angle of approximately  $10^\circ$  compared to *ca.*  $4^\circ$  in  $\beta$ -1, (Fig. S1 in ESI†). The pseudo Jahn-Teller axis is unvaried from  $\beta$ -1, the Cu–O bond remaining the longest (Cu–O 2.360(12), Cu–N 2.01(2), Cu–F 1.885(5) Å). Therefore, phase transition IV is not the consequence of an orbital reordering. This is confirmed by periodic density functional calculations<sup>7</sup> that indicate spin density accumulation on Cu (0.75), on each F (0.05) and on each pyz (0.12 overall), see Fig. S6 in the ESI.† No transformation of  $\epsilon$ -1 was observed, at least up to 4.4 GPa, indicating that the  $\text{H}_2\text{O--Cu--OH}_2$  direction remains the elongated one up to this pressure. The hydrogen bond pattern is similar to those of phases  $\alpha$ – $\gamma$  (Fig. 1) and the  $\text{H}_2\text{O}\cdots\text{F}$  distances are comparable to those of  $\beta$ -1. Therefore, the magnetic exchange interactions must be 1D, in analogy with  $\beta$ -1.<sup>2</sup>

Complementary P-XRD measurements confirmed the occurrence of phase transition IV above 3.2 GPa, though always concomitant with transition II, making phases  $\beta$ ,  $\gamma$  and  $\epsilon$  co-existing up to 3.8 GPa. None of these experiments gave any unambiguous evidence of  $\delta$ -1, so far obtained only from the single crystal experiments by

Table 1 Selected crystallographic information on the polymorphs of **1** and **2**

Phase name	$\alpha$ -1	$\beta$ -1	$\gamma$ -1	$\delta$ -1	$\epsilon$ -1	<b>2</b>
Crystal system		Monoclinic		Triclinic	Triclinic	Monoclinic
Space group, $Z^a$		$P2_1/c$ , 2		$A\bar{1}$ , 3	$A\bar{1}$ , 2	$I2/c$ , 4
Technique		P-XRD		SC-XRD	SC-XRD	SC-XRD
$P$ (GPa)	0.0001	1.1	3.8	3.3	3.3	0.0001
Unit cell dimensions:						
$a$ (Å)	7.6893(3)	6.8703(4)	6.8112(6)	6.7987(8)	6.813(4)	21.0200(3)
$b$ (Å)	7.5655(1)	7.6758(1)	7.6632(6)	10.452(6)	7.1823(11)	7.55300(10)
$c$ (Å)	6.9001(3)	7.1103(5)	6.5422(8)	7.272(2)	7.4463(12)	6.88100(10)
$\alpha$ (°)	90	90	90	86.24(3)	84.344(15)	90
$\beta$ (°)	111.205(5)	114.108(7)	117.318(10)	115.844(16)	116.72(4)	98.456(2)
$\gamma$ (°)	90	90	90	88.71(2)	78.85(3)	90
$V$ (Å <sup>3</sup> )	374.22(3)	342.25(4)	303.39(6)	463.3(3)	312.1(2)	1080.58(3)
$V_{\text{mol}}$ (cm <sup>3</sup> mol <sup>-1</sup> )	112.70	103.07	91.37	93.02	93.99	162.71
Reference	This study	This study	This study	3	This study	This study

<sup>a</sup>  $Z$  is intended as the number of the corresponding  $[(\text{CuF}_2(\text{H}_2\text{O})_2)_x(\text{pyz})]$  formula units per unit cell.



Prescimone *et al.*<sup>3</sup> The simultaneous occurrence of three phase changes (II, III and IV) is thermodynamically forbidden, therefore kinetic effects must play an important role during these transformations. In fact, we found that larger pressure increase rates favor  $\gamma$ -1, which was the only product when the pressure was directly increased to 3.8 GPa. The purity of this sample enabled us to refine its structure from P-XRD data using a more flexible model (see the ESI† for details). The elongation of Cu–F proposed by Halder *et al.*<sup>2</sup> was confirmed (2.215(16) Å), in agreement with periodic DFT calculations (2.198 Å) and the spin density maps prove the re-orientation of the magnetic orbital (see Fig. S5, ESI†), which does not involve F atoms.

The surprising behavior of **1** is complemented by the discovery of  $[(\text{CuF}_2(\text{H}_2\text{O})_2)(\text{pyz})]$  (**2**, Fig. 3), obtained for the first time as a second crystalline fraction from several solutions under ambient conditions. **2** was also found to grow epitaxially on large crystals of **1** stored in their mother liquor. The crystal structure of **2** is monoclinic *I2/c* (ref. 6) and comprises one moiety of  $[\text{CuF}_2(\text{H}_2\text{O})_2(\text{pyz})_{0.5}]$  in the asymmetric unit. One pyz, two  $\text{F}^-$  and three  $\text{H}_2\text{O}$  molecules coordinate to the  $\text{Cu}^{2+}$  centers in a distorted octahedral fashion. The pseudo Jahn–Teller axis is N–Cu–O<sub>bridge</sub> suggesting that the magnetic orbital is located in the  $\text{CuF}_2\text{O}_2$  plane as in  $\alpha$ -1 (Cu–O 2.5210(13), Cu–N 2.4041(15), Cu–O' 1.9922(13), Cu–O'' 1.9653(14), Cu–F 1.8987(10), and Cu–F' 1.8936(10) Å). Two  $\text{H}_2\text{O}$  molecules act as bridges in the equatorial-axial position between the Cu ions, thus building pairs of edge-sharing distorted octahedra (Fig. S5, ESI†). Overall, a 1D coordination polymer, extended along the crystallographic *a* axis, is formed in which each pyz links two  $\text{Cu}_2\text{F}_4(\text{H}_2\text{O})_4$  dimeric moieties (Fig. 3). The N–Cu–OH<sub>2</sub> bond is slightly tilted with respect to the translational direction of the polymer. The aromatic rings assume alternate orientations along the same chain. As for **1**, the chains of **2** are packed in a 2D supramolecular network of H-bonds in the *bc* plane which involves all the water and the fluoride ligands (Fig. S7c, ESI†) with  $\text{H}_2\text{O} \cdots \text{F}$  distances comparable to those of  $\alpha$ -1. Table 1 summarizes relevant crystallographic information.

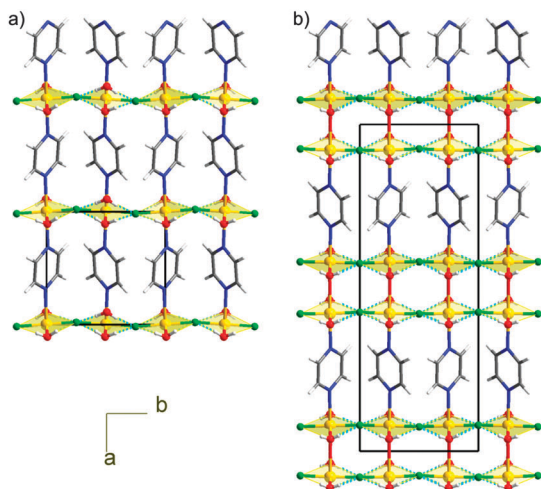


Fig. 3 Comparison of the crystal packing for  $\alpha$ -1 (a) and **2** (b). In both cases, the magnetic, H-bond-mediated single layers (for **1**) or thick bilayers (for **2**) are perpendicular to the polymeric chains and therefore to the plane of the picture.

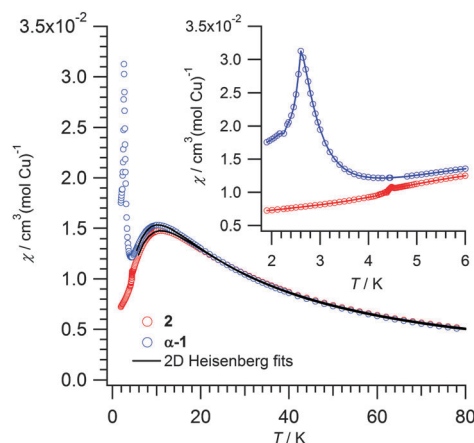


Fig. 4 Magnetic susceptibility of **2** (red) and  $\alpha$ -1 (blue) in the deuterated form. The black lines represent the respective 2D Heisenberg antiferromagnetic fits. The low temperature region (inset) shows a peak at 4.5 K for **2** and at 2.6 K for  $\alpha$ -1 due to long range ordering.

The magnetic susceptibility  $\chi$  of **2** (in deuterated form) shows a broad maximum at 11 K, due to short range antiferromagnetic correlations. At lower *T*,  $\chi$  declines and features a faint peak at 4.5 K. In comparison,  $\chi$  of  $\alpha$ -1 has a broad maximum at 10.5 K and a sharp peak at 2.6 K (Fig. 4). At 250 K,  $\chi T$  is 0.478 and 0.458  $\text{emu K mol}^{-1}$  for **2** and  $\alpha$ -1, respectively, both higher than the spin-only moment of  $\text{Cu}^{2+}$  ( $g = 2$ ; 0.375  $\text{emu K mol}^{-1}$ ). For both **2** and  $\alpha$ -1,  $\chi T$  declines with decreasing *T*, slightly until 60 K and more significantly thereafter (Fig. S8, ESI†). Curie–Weiss fits result in negative Weiss  $\theta$  values, confirming the dominant antiferromagnetic interactions (Table 2).

Both compounds exhibit 2D  $\text{Cu}^{2+}$  layers, hence it is adequate to characterize them as spin 1/2 Heisenberg square lattices, with the Hamiltonian  $H = -J_{ij} \sum S_i \cdot S_j$ . The results of the fitting for these quantum Heisenberg antiferromagnets are shown in Table 2. Fitted *J* values are consistent with the mean-field expression  $|2k_B T_{\text{max}}/JS(S+1)| = 2.53$ ,<sup>8</sup> that would predict  $|J| = 11.6$  K and 11.1 K for **2** and  $\alpha$ -1, respectively, as well as with the literature values reported for  $\alpha$ -1.<sup>1b</sup> Since the 2D network is similar, it is reasonable to find comparable exchange parameters **2** and  $\alpha$ -1. Further proof of the robustness of this H-bonded network is given by  $\text{CuF}_2(\text{H}_2\text{O})_2(3\text{-chloropyridine})$ .<sup>8</sup> As shown in Fig. 5, the peak at 4.5 K in the magnetic susceptibility of **2** is gradually suppressed by the increasing field, which is typical for spin-canting,<sup>8</sup> whereas the broad maximum at 11 K is field-independent. The steep decline of  $\chi$  below the peak can be understood as an antiferromagnetic order between the bi-layers. In  $\alpha$ -1 long range order (LRO) is observed at 2.6 K.<sup>1b</sup> The higher LRO temperature of **2** can be regarded as a consequence of the bi-layer present in **2** and distinct from  $\alpha$ -1. Indeed bridging water molecules occupying equatorial-axial

Table 2 Selected magnetic parameters of **2** and  $\alpha$ -1

Compound	$\theta^a$ (K)	$g^b$	$J^b$ (K)	$T_N$ (K)
<b>2</b>	−17.3(1)	2.22(1)	11.75(5)	4.5
$\alpha$ -1	−15.6(1)	2.18(1)	10.99(5)	2.6

<sup>a</sup> Curie–Weiss fit between 35–250 K. <sup>b</sup> 2D Heisenberg fit.



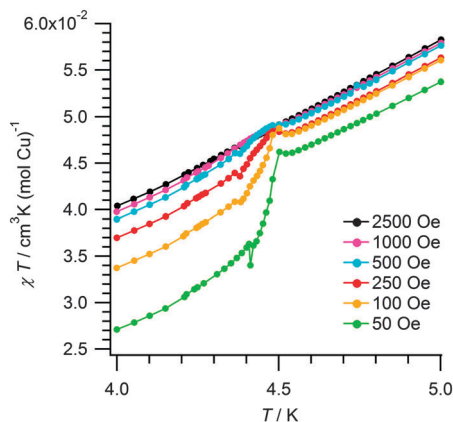


Fig. 5 Magnetic field dependence of the ordering temperature in **2**.  $\chi T$  vs.  $T$  measured at different fields.

positions have been found to cause small magnetic coupling, but were seldom studied before.<sup>9</sup>

This study demonstrates that the  $[(\text{CuF}_2(\text{H}_2\text{O})_2)_x(\text{pyz})]$  system has an even richer phase diagram than reported so far. A new high-pressure polymorph,  $\epsilon$ -1, was discovered and structurally characterized and the structure of  $\gamma$ -1 was better elucidated. Interestingly, **1** is now known to form three different phases at the same pressure (*ca.* 3.3 GPa). Such abundance of easily accessible polymorphs implies very similar free energies and important kinetic effects. Preliminary experiments using different pressure increase rates and equilibration times, indicate that  $\epsilon$ -1 forms only when compressed under quasi-reversible conditions, whereas  $\gamma$ -1 is the only product if the compression is very rapid.<sup>10</sup> On the other hand, the fact that  $\delta$ -1 was not reproduced by us under any experimental conditions suggests that the more radical transformation III might not be stimulated only by pressure. Depending on the conditions,  $[\text{CuF}_2(\text{H}_2\text{O})_2(\text{pyz})]$  rapidly gives crystalline  $[\text{CuF}_2(\text{pyz})]$ ,<sup>11</sup> thus  $\delta$ -1 could be regarded as an intermediate of a dehydration reaction, in which one of the water molecules, replaced by  $\text{F}^-$ , leaves the Cu coordination sphere but remains trapped in the crystal. Noteworthy, the experiment by Prescimone *et al.*<sup>3</sup> was carried out on a single crystal, where the dehydration might have occurred more slowly especially if the sample was kept under pressure.

Another outcome of our study is the discovery of compound **2**, which is complementary to  $\delta$ -1 and  $\text{CuF}_2(\text{H}_2\text{O})_2$ ,<sup>12</sup> having water instead of fluorine bridges. **2** differs from **1** in the stoichiometry, and the main structural difference is the alternation of pyz and double (instead of single)  $\text{Cu}(\text{H}_2\text{O})_2\text{F}_2$  layers linked by bridging water molecules. **2** is a 2D Heisenberg

antiferromagnet and the bi-layer feature results in a higher LRO temperature.

Further investigations are currently in progress in order to analyze the role of kinetics, radiation exposure and sample preparation in triggering the alternative phase transitions and reactions. Moreover, the high-pressure behavior of **2** and its magnetic structure are currently being investigated.

We thank Dr. Vincent Olieric for the help in performing the P-XRD experiments at X06DA in a non-conventional setup and Urs Kämpfer for the elemental analysis. The Swiss National Science Foundation supported this research under projects 144534, 132877, and 150257.

## Notes and references

- (a) M. Conner, A. McConnell, J. Schlueter and J. Manson, *J. Low Temp. Phys.*, 2006, **142**, 273; (b) J. L. Manson, M. M. Conner, J. A. Schlueter, A. C. McConnell, H. I. Southerland, I. Malfant, T. Lancaster, S. J. Blundell, M. L. Brooks, F. L. Pratt, J. Singleton, R. D. McDonald, C. Lee and M.-H. Whangbo, *Chem. Mater.*, 2008, **20**, 7408; (c) J. A. Schlueter, H. Park, J. L. Manson, H. Nakotte and A. J. Schultz, *Phys. B*, 2010, **405**, S324; (d) J. L. Musfeldt, Z. Liu, S. Li, J. Kang, C. Lee, P. Jena, J. L. Manson, J. A. Schlueter, G. L. Carr and M. H. Whangbo, *Inorg. Chem.*, 2011, **50**, 6347; (e) C. H. Wang, M. D. Lumsden, R. S. Fishman, G. Ehlers, T. Hong, W. Tian, H. Cao, A. Podlesnyak, C. Dunmars, J. A. Schlueter, J. L. Manson and A. D. Christianson, *Phys. Rev. B*, 2012, **86**, 064439; (f) S. Ghannadzadeh, J. S. Moeller, P. A. Goddard, T. Lancaster, F. Xiao, S. J. Blundell, A. Maisuradze, R. Khasanov, J. L. Manson, S. W. Tozer, D. Graf and J. A. Schlueter, *Phys. Rev. B*, 2013, **87**, 241102.
- G. J. Halder, K. W. Chapman, J. A. Schlueter and J. L. Manson, *Angew. Chem., Int. Ed.*, 2011, **50**, 419.
- A. Prescimone, C. Morien, D. Allan, J. A. Schlueter, S. W. Tozer, J. L. Manson, S. Parsons, E. K. Brechin and S. Hill, *Angew. Chem., Int. Ed.*, 2012, **51**, 7490.
- We propose a homogeneous labelling of the phases of **1**, based on the use of greek letters, as is common use for identifying polymorphs.
- L. R. Falvello, *J. Chem. Soc., Dalton Trans.*, 1997, 4463.
- The non-conventional crystallographic setting was chosen in order to allow straightforward comparison of the new phase with the other crystal structures.
- R. Dovesi, V. R. Saunders, C. Roetti, R. Orlando, C. M. Zicovich-Wilson, F. Pascale, B. Civalleri, K. Doll, N. M. Harrison, I. J. Bush, P. D'Arco and M. Llunell, *CRYSTAL09 User's Manual*, University of Torino, Torino, 2009.
- S. H. Lapidus, J. L. Manson, H. Park, A. J. Clement, S. Ghannadzadeh, P. Goddard, T. Lancaster, J. S. Möller, S. J. Blundell, M. T. F. Telling, J. Kang, M.-H. Whangbo and J. A. Schlueter, *Chem. Commun.*, 2013, **49**, 499.
- D. Ghoshal, T. K. Maji, G. Mostafa, S. Sain, T. H. Lu, J. Ribas, E. Zangrando and N. R. Chaudhuri, *Dalton Trans.*, 2004, 1687.
- M. Fisch, A. Lanza, N. Casati and P. Macchi, in preparation.
- S. H. Lapidus, J. L. Manson, J. Liu, M. J. Smith, P. Goddard, J. Bendix, C. V. Topping, J. Singleton, C. Dunmars, J. F. Mitchella and J. A. Schlueter, *Chem. Commun.*, 2013, **49**, 3558.
- (a) S. C. Abrahams and E. Prince, *J. Chem. Phys.*, 1962, **36**, 50; (b) S. C. Abrahams, *J. Chem. Phys.*, 1962, **36**, 56.

